Mathematical modeling suggests cytotoxic T lymphocytes control growth of B16 tumor cells in collagin-fibrin gels by cytolytic and non-lytic mechanisms

Barun Majumder, Sadna Budhu, John D. Loike, Samuel C. Silverstein, Vitaly V. Ganusov

Supplemental Information

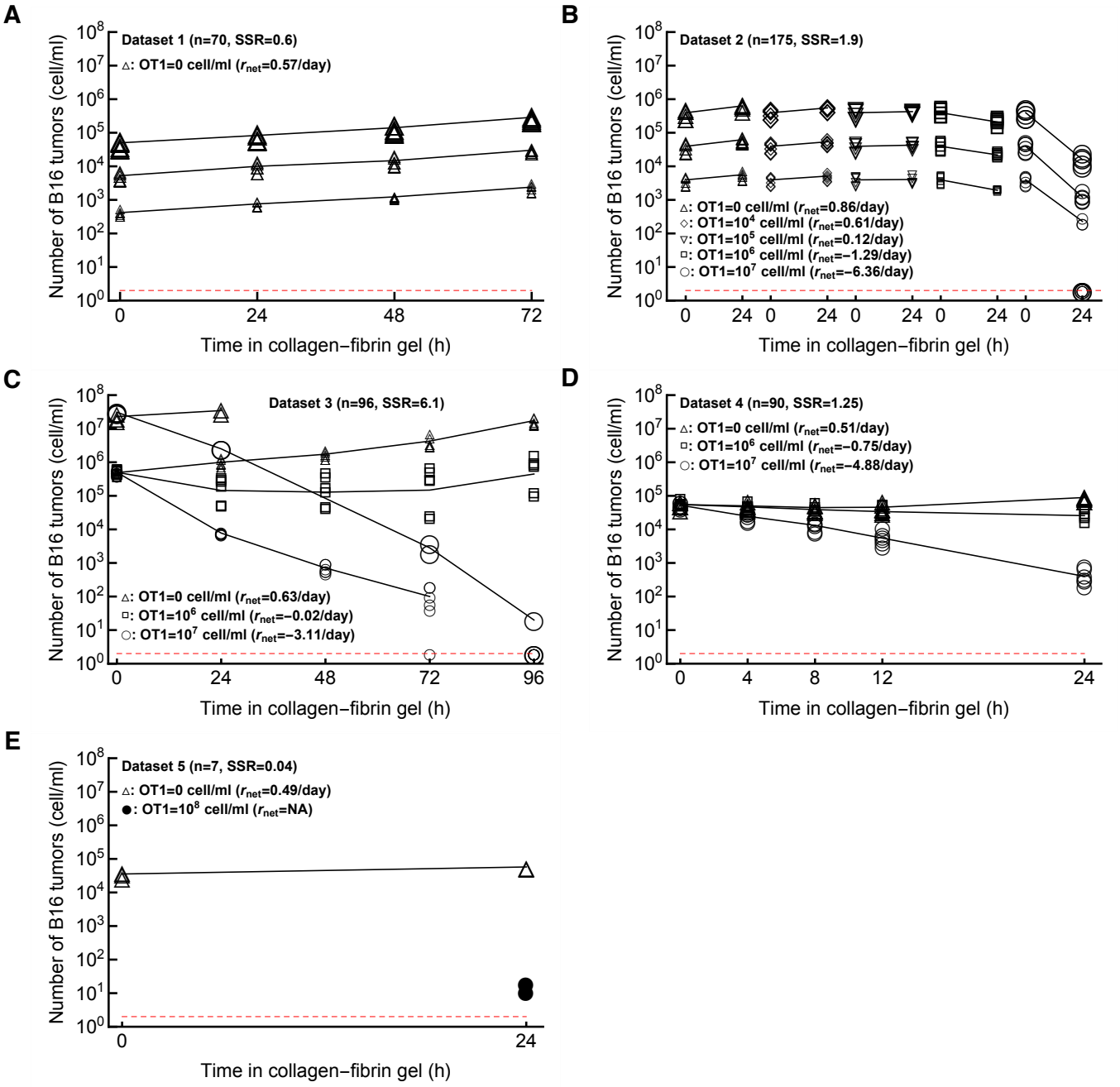

Supplemental Figure S1: Data on the dynamics of B16 tumor cells for different time periods and at different CTL concentrations. We show all 5 datasets (Dataset 1-5, panels A-E) analyzed in this paper. (A) **Dataset 1** (no CTLs) is on B16 tumor growth for 72 hours in the absence of CTLs; (B) **Dataset 2** is on B16 tumor dynamics for 24 hours at different initial B16 cell and CTL concentrations (note that 5 gels had 0 B16 cells recovered, all at OT1= 10^7 cells/ml); (C) **Dataset 3** is on B16 tumor dynamics for up to 96 hours at different initial B16 cell and CTL concentrations (note that 8 gels had 0 B16 cells recovered at 72 and 96 hours post inoculation); (D) **Dataset 4** on B16 tumor dynamics in the first 24 hours after inoculation at 3 different CTL concentrations, and (F) **Dataset 5** (high CTL density) on B16 tumor dynamics for 24 hours at 0 and 10^8 OT1 cells/ml. The size of markers indicates the different targeted number of B16 tumor cells. The lines connect average numbers (excluding gels with 0 B16 cells in B&C). For each panel we also show the number of gels n and sum of squared residuals (SSR) are computed by the relation $\text{SSR} = \sum_{i=1}^{N}(y_i - \bar{y}_t)^2$. The red horizontal dashed line is the limit of detection for the experiments set at 2 cells/ml.

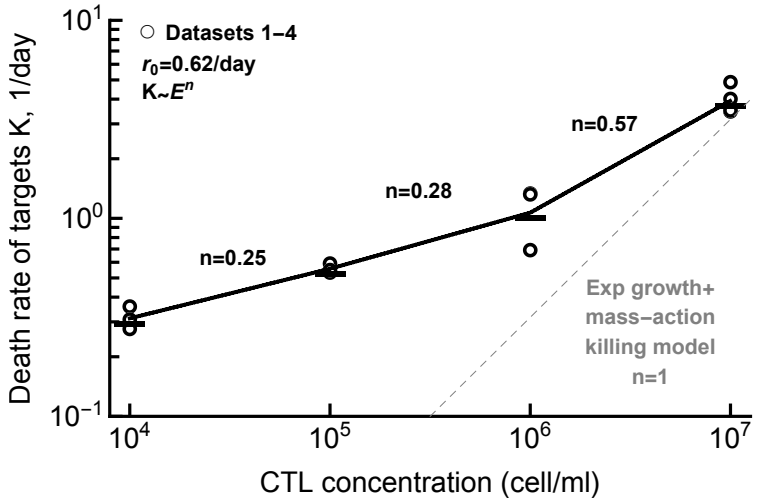

Supplemental Figure S2: Regression analysis suggests nonlinear change of the death rate of B16 tumor cells with increasing CTL concentration. For the data in Datasets 1-4 we estimated the net rate of growth of B16 tumor cells over time r_{net} for every CTL and targeted B16 tumor concentrations (see **Supplemental Figure S1** for the average r_{net} per CTL concentration). In the absence of CTLs, the net growth rate of tumors was $r_{\text{net}} = r_0 = 0.62/\text{day}$. We then calculated the death rate of B16 tumor cells K by substracting the estimated net rate of tumor change from r_0, $K = r_0 - r_{\text{net}}$. Individual symbols are estimates of K for different target B16 tumor concentrations at a given CTL level. Assuming that death rate depends on CTL concentration as powerlaw with scale n, we estimated n for individual ranges of CTL concentrations. For example, the death rate of targets scales as $K \sim E^{0.25}$ for CTL concentrations E between 10^4 and 10^5 cells/ml. The dashed line shows a linear relationship $K \sim E$ between the death rate of targets K and CTL concentration E as predicted by the exponential-growth-mass-action-killing model (eqn. (3)).

Datasets 1-5 ($E \leq 10^8$ cell/ml): n=438												
Model	α	r, **1/day**	k	h	n	g_0	g_1	g_2	**SSR**	**AIC**	**ΔAIC**	**w**
MA	2.78	0.24	1.85×10^{-7}						779	1503	779	0
Sat	2.81	0.696	7.32	8.63×10^6					131	724	0	1
Power	2.78	0.792	0.0017		0.477				147	776	52	0
SiGMA	2.95		1.72×10^{-7}			2.88×10^{-8}	0.86	291	583	1380	656	0

Supplemental Table S1: The model with exponential growth of tumors and saturated killing rate by CTLs gives the best fit when the models are fitted to all data (Datasets 1-5). We list the best-fit parameters for the alternative models along with SSR, AIC, ΔAIC and Akaike weights w. Other details are similar to those given in **Table 1**.

	SiGMA model Datasets 1-4 ($n = 431$)		**Sat model Datasets 1-4** ($n = 438$)	
Parameters	**Fixed** α	**Varied** α	**Fixed** α	**Varied** α
α	**2.71**		**2.82**	
α_1		**3.18**		**2.89**
α_2		**2.7**		**2.82**
α_3		**2.74**		**2.86**
α_4		**2.49**		**2.64**
α_5		**3.85**		**3.56**
r			**0.7**	**0.7**
k	**3.29**$\times 10^{-7}$	**3.24**$\times 10^{-7}$	**7.2**	**7.2**
h			8.64×10^6	**8.14**$\times 10^6$
g_0	**0.12**	**0.096**		
g_1	**0.65**	**0.67**		
g_2	**6714**	**6382**		
AIC	**654.2**	**650.5**	**723.7**	**727.5**
LR	**11.8**		**4.3**	
χ**(0.95,4)**	**9.5**		**9.5**	
p	**0.02**		**0.37**	

Supplemental Table S2: Assuming different scaling factors α in best fit models moderately improves the fit but results in similar parameter estimates. We fitted the SiGMA model (eqn. (6)) to the data from Datasets 1-4 or the Sat model (eqn. (4)) to the data from Datasets 1-5 with one or five different scaling factors α.

Datasets 1-4 (subset) $n = 371$												
Models	α	**r**	**k**	**h**	**n**	g_0	g_1	g_2	**SSR**	**AIC**	**ΔAIC**	**w**
MA	**2.88**	**0.72**	**3.84**$\times 10^{-7}$						**88**	**526**	**99.7**	**0**
Sat	**2.74**	**0.72**	**4.8**	**2.49**$\times 10^{6}$					**71**	**451**	**24.7**	10^{-6}
Power	**2.67**	**0.74**	**0.004**		**0.423**				**66.7**	**426.3**	**0**	**0.93**
SiGMA	**2.68**		**3.17**$\times 10^{-7}$			**6.84**$\times 10^{-8}$	**0.72**	**7930**	**67.3**	**431.4**	**5.1**	**0.072**
Datasets 1-5 (subset) $n = 378$												
Models	α	**r**	**k**	**h**	**n**	g_0	g_1	g_2	**SSR**	**AIC**	**ΔAIC**	**w**
MA	**2.85**	**0.32**	**1.87**$\times 10^{-7}$						**724**	**1327**	**889**	**0**
Sat	**2.86**	**0.72**	**9.36**	**1.39**$\times 10^{7}$					**82**	**503**	**65**	**0**
Power	**2.62**	**0.72**	**0.01**		**0.37**				**69**	**438**	**0**	**1**
SiGMA	**2.94**		**1.76**$\times 10^{-7}$			**1.18**$\times 10^{-7}$	**0.84**	**252**	**544**	**1222**	**784**	**0**

Supplemental Table S3: A phenomenological Power model gives the best fit for the subset of the data. B16 tumor dynamics in two settings (at $T = 10^6$ cell/ml and $E = 10^6$ cell/ml from Dataset 3 and $T = 10^5$ cell/ml and $E = 10^6$ cell/ml from Dataset 4) is not monotonic (**Supplemental Figure S1**). We fitted 4 alternative models (eqns. (3)–(6)) to the subset of the data that excludes these two settings for Datasets 1-4 (top) or Datasets 1-5 (bottom). Other details are similar to those given in **Table 1**.

Datasets 1-4	B16 = 10^4	$n = 80$										
Models	α	**r**	**k**	**h**	**n**	g_0	g_1	g_2	**SSR**	**AIC**	**ΔAIC**	**w**
MA	**2.74**	**0.6**	**3.55**$\times 10^{-7}$						**14**	**96**	**60.5**	**0**
Sat	**2.67**	**0.62**	**4.08**	**1.85**$\times 10^{6}$					**8**	**54**	**18.5**	10^{-4}
Power	**2.46**	**0.65**	**0.009**		**0.37**				**6.4**	**35.5**	**0**	**0.99**
SiGMA	**2.52**		**2.93**$\times 10^{-7}$			**1.2**$\times 10^{-7}$	**0.67**	**8162**	**7.5**	**50**	**14.5**	10^{-3}
Datasets 1-4	B16 = 10^5	$n = 142$										
Models	α	**r**	**k**	**h**	**n**	g_0	g_1	g_2	**SSR**	**AIC**	**ΔAIC**	**w**
MA	**2.42**	**0.53**	**4.63**$\times 10^{-7}$						**20**	**134**	**36.65**	**0**
Sat	**2.36**	**0.58**	**6.48**	**4.07**$\times 10^{6}$					**16.5**	**107**	**9.65**	**4.2**$\times 10^{-3}$
Power	**2.33**	**0.58**	**0.001**		**0.52**				**15.37**	**97.35**	**0.17**	**0.48**
SiGMA	**2.34**		**4.1**$\times 10^{-7}$			**1.37**$\times 10^{-7}$	**0.6**	**7322**	**15.14**	**97.18**	**0**	**0.52**
Datasets 1-5	B16 = 10^5	$n = 149$										
Models	α	**r**	**k**	**h**	**n**	g_0	g_1	g_2	**SSR**	**AIC**	**ΔAIC**	**w**
MA	**3.34**	**0.38**	$\times 10^{-7}$						**175**	**454**	**336.6**	**0**
Sat	**2.4**	**0.55**	**9.12**	**9.6**$\times 10^{6}$					**18**	**117.4**	**0**	**1**
Power	**2.35**	**0.62**	**0.02**		**0.33**				**22**	**149**	**31.6**	**0**
SiGMA	**2.96**		**9.38**$\times 10^{-8}$			**1.38**$\times 10^{-7}$	**0.9**	**6106**	**139**	**425**	**307.6**	**0**
Datasets 1-5	B16 = 10^6	$n = 112$										
Models	α	**r**	**k**	**h**	**n**	g_0	g_1	g_2	**SSR**	**AIC**	**ΔAIC**	**w**
MA	**3.16**	**0.89**	**3.79**$\times 10^{-7}$						**28**	**170**	**39**	**0**
Sat	**2.93**	**0.89**	**4.56**	**2.1**$\times 10^{6}$					**21.5**	**143**	**12**	**2**$\times 10^{-3}$
Power	**2.8**	**0.89**	**0.008**		**0.39**				**19.36**	**131**	**0**	**0.82**
SiGMA	**2.8**		**2.95**$\times 10^{-7}$			**9.8**$\times 10^{-8}$	**0.9**	**10243**	**19.43**	**134**	**3**	**0.18**

Supplemental Table S4: The Power model fits the subset of data best when we focus on a single targeted B16 tumor cell concentration in the gel. Here we divided Datasets 1-4 (top) or Datasets 1-5 (bottom) based on the target B16 concentration. For $T = 10^4$ and 10^6, the Power model provides the best fit. For $T = 10^5$ without the high CTL data (Datasets 1-4), both the SiGMA and the Power model fits the data with similar Akaike weights. However, if we include the high CTL data (Datasets 1-5), the Sat model best explains the data. For other details of the table refer to **Table 1**.

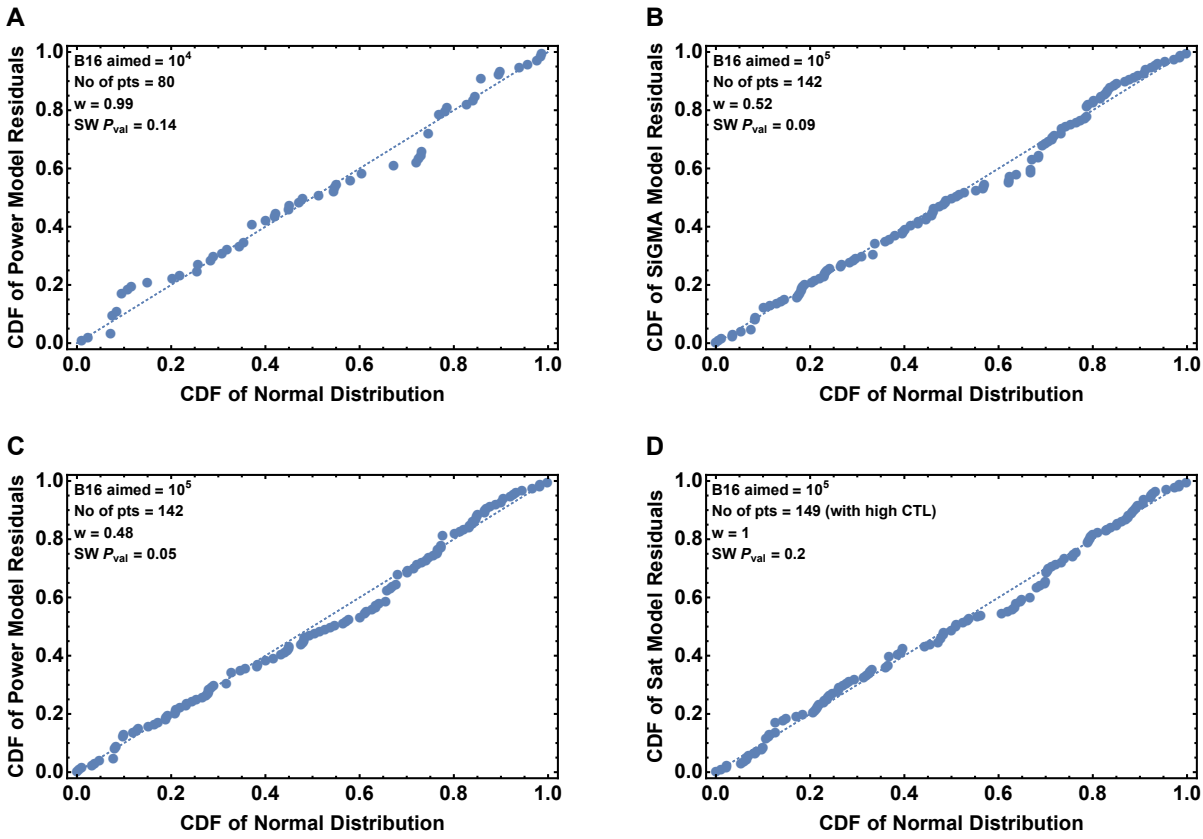

Supplemental Figure S3: The residuals of the best models for sub-datasets with $T = 10^4$ and 10^5 are normally distributed. Here we show the normal probability plot of the best models of **Table S4** for $T = 10^4$ (A) and 10^5 (B,C,D) with the p-value of the Shapiro-Wilk (SW) test.

Experiment 1	**dataset**	$n = 125$										
Models	α	**r**	**k**	**h**	**n**	g_0	g_1	g_2	**SSR**	**AIC**	**ΔAIC**	**w**
MA	**2.57**	**0.65**	**3.84**$\times 10^{-7}$						**34**	**201**	**27**	**0**
Sat	**2.44**	**0.67**	**4.75**	**2.26**$\times 10^{6}$					**27.8**	**177**	**3**	**0.18**
Power	**2.39**	**0.67**	**0.003**		**0.44**				**27.15**	**174**	**0**	**0.8**
SiGMA	**2.43**		**3.22**$\times 10^{-7}$			**9.6**$\times 10^{-8}$	**0.7**	**12726**	**28.4**	**182**	**8**	**0.015**
Experiment 2	**dataset**	$n = 126$										
Models	α	**r**	**k**	**h**	**n**	g_0	g_1	g_2	**SSR**	**AIC**	**ΔAIC**	**w**
MA	**3.47**	**0.84**	**3.84**$\times 10^{-7}$						**32**	**191**	**29.2**	**0**
Sat	**3.32**	**0.86**	**4.8**	**2.78**$\times 10^{6}$					**27**	**174**	**12.2**	**0.002**
Power	**3.2**	**0.86**	**0.005**		**0.42**				**25**	**164**	**2.2**	**0.25**
SiGMA	**3.18**		**3.07**$\times 10^{-7}$			**0.018**	**0.84**	**6448**	**24.2**	**161.8**	**0**	**0.75**
Experiment 3	**dataset**	$n = 120$										
Models	α	**r**	**k**	**h**	**n**	g_0	g_1	g_2	**SSR**	**AIC**	**ΔAIC**	**w**
MA	**2.69**	**0.67**	**3.84**$\times 10^{-7}$						**18**	**121**	**61.6**	**0**
Sat	**2.55**	**0.7**	**4.8**	**2.45**$\times 10^{6}$					**12.5**	**79.5**	**20.1**	**0**
Power	**2.47**	**0.7**	**0.005**		**0.41**				**10.6**	**59.4**	**0**	**0.86**
SiGMA	**2.50**		**3.22**$\times 10^{-7}$			**1.08**$\times 10^{-7}$	**0.72**	**8650**	**10.76**	**63**	**3.6**	**0.14**

Supplemental Table S5: The Power and the SiGMA models give the best fit if we fit the models to subsets of data experiment-wise. As we described in Materials and methods, each Datasets 1-4 has three experiments performed in duplicates. If we divide the data based on the three Experiments 1, 2 and 3 then the Power model gives the best fit for Experiment 1 and 3. For Experiment 2, the SiGMA model gives the best fit. The description of the table remain same as that of **Table 1**.

A	Dataset 4	$n = 90$										
Models	α	**r**	**k**	**h**	**n**	g_0	g_1	g_2	**SSR**	**AIC**	**ΔAIC**	**w**
MA	**1.94**	**0.048**	**4.78**$\times 10^{-7}$						**9.67**	**63**	**11.5**	**0**
Sat	**1.94**	**0.31**	**8.64**	**7.42**$\times 10^{6}$					**8.35**	**51.5**	**0**	**0.5**
Power	**1.94**	**0.31**	**8.16**$\times 10^{-5}$		**0.68**				**8.35**	**51.5**	**0**	**0.5**
SiGMA	**1.94**		**4.75**$\times 10^{-7}$			**6.98**$\times 10^{-9}$	**0.23**	**445106**	**9.26**	**63**	**11.5**	**0**

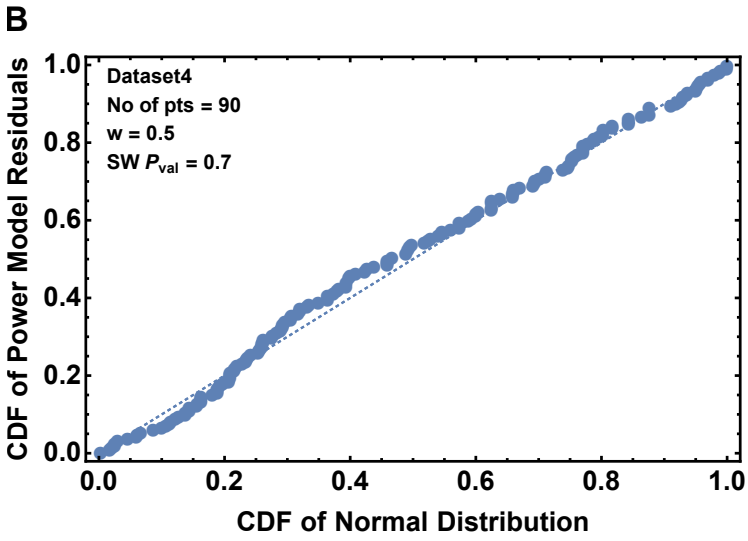

Supplemental Figure S4: The phenomenological Power and the Sat models equally well describe the data for Dataset 4. Dataset 4 describes dynamics of B16 tumor cells within first 24 hours after inoculation into collagen-fibrin gels and has $n = 90$ data points. Parameter estimates are shown in panel A, and q-q plot for the the residuals for the models is shown in panel B. The table details in (A) are similar to **Table 1**.

Dataset 4	**OT1=0**	$n = 30$								
Models	α	**r**	**t'**	**d**	f_d	**SSR**	**AIC**	**ΔAIC**	**w**	**SW** p
EG	**2.22**	**0.5**				**2.24**	**13.4**	**12.8**	**0**	**0.46**
Alt 1	**2.48**	**1.13**	**8**			**1.37**	**0.6**	**0**	**0.59**	**0.6**
Alt 2	**1.79**	**3.12**		**1.03**	**0.95**	**1.3**	**1.3**	**0.7**	**0.41**	**0.43**

Supplemental Table S6: Both the alternative models fit the data better than the EG model for the growth only subset of the data in the Dataset 4. We selected the data on B16 tumor growth with OT1=0 resulting in $n = 30$ data points and fitted the EG, Alt 1, and Alt 2 models (eqn. (3) and eqns. (8)–(9), respectively) to these data (see **Figure 4**B for model fits). We show the results of the Shapiro-Wilk (**SW**) normality test of the residuals. Other details are similar to those in **Table 1**.

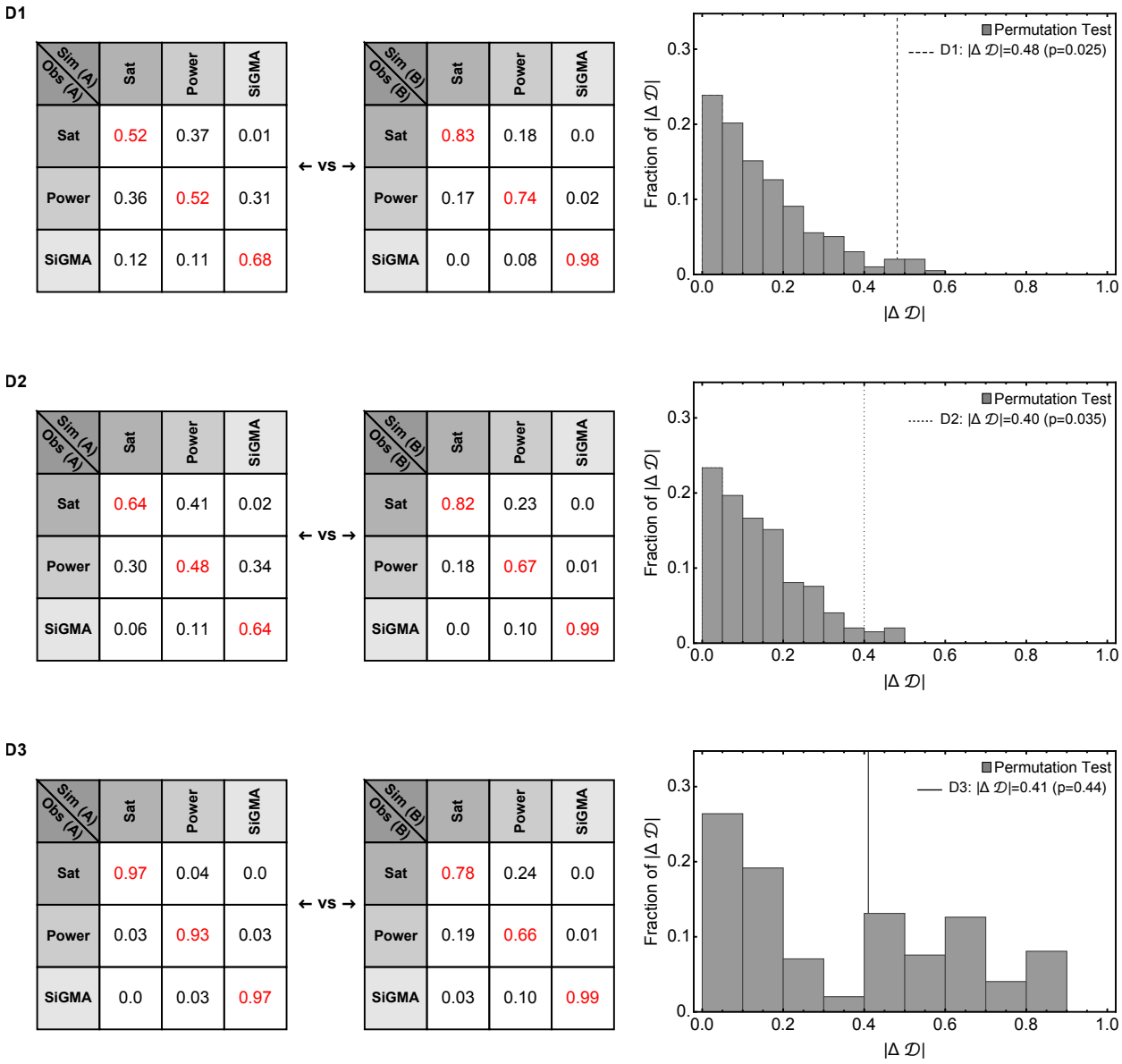

Supplemental Figure S5: Statistical power to detect a difference in the fit quality between alternative mathematical models depends on experimental design. We performed simulations of 3 experimental designs measuring impact of CTLs on B16 tumor dynamics (see **Figure 5** and Main text for details). For designs D1 and D2 we show that the experiment type A and B are significantly different from each other. With permutation test, however, for D3 we fail to reject the null hypothesis that the experiments are similar. For three simulated experimental designs D1, D3 and D3 we simulated 100 identical replicas for investigation Type A and B from a model while choosing the errors randomly and then fitted them with models. This allowed us to get matrices like the ones in the left 2 panels. The red diagonal entries show fraction of replicas generated by the a model is also best fitted by the same model where as the off diagonal entries present fraction of replicas generated by a model but best fitted by a different model. The experimental Type A or B with heavier diagonal terms would indicate a better experiment. In this plot we did a permutation test to compare the observed $|\Delta\mathcal{D}|_{\text{obs}}$ in a permutated distribution of $|\Delta\mathcal{D}|_{\text{per}}$ to obtain a p-value, where $\mathcal{D}$ is a determinant of the matrices. This test allowed us to statistically comment on the structural difference of the design Types A and B. The details of the test is discussed in the end of Results section. See eqn. (12) for test statistic measure.